

Results from Cascade Thrust Reverser Noise and Suppression Experiments

Orlando A. Gutierrez,* James R. Stone,†
and Robert Friedman‡

NASA Lewis Research Center, Cleveland, Ohio

Results are presented from experimental work on model scale cascade reversers with cold airflow. Sound power level directivity and spectral characteristics for cascade reversers are reported. Effect of cascade exit area ratio, vane profile shape, and emission arc are discussed. Model equivalent diameters varied from 3-5 in.; pressure ratios ranged from 1.15-3.0. Depending on the reverser type, acoustic power was proportional to the $4\frac{1}{2}$ -6th power of ideal jet velocity. Reverser noise peaked at higher frequency and was more omnidirectional than nozzle-alone jet noise. Appreciable reduction in sideline noise was obtained from plane shields. Airfoil-vaned cascades were the most aerodynamically efficient and least noisy reversers. Scaling of cascade reverser data to example aircraft engines showed all cascades above the 95 PNdb sideline goal for STOL aircraft. However, the airfoil-vaned reverser has a good potential for meeting this goal for high bypass (low pressure ratio) exhausts.

Nomenclature

A_e	= equivalent flow area of cascade, $A_e \equiv \dot{m}/U_j$, in. ²
A_{ex}	= total exit flow area of cascade assembly in direction of vane exit angle
A'_{ex}	= exit flow area of each cascade vane passage, in. ²
A_{in}	= total flow area in duct ahead of cascade assembly, in. ²
A'_{min}	= minimum flow area of each cascade vane passage, in. ²
c	= cascade vane chord, in.
c_o	= speed of sound at atmospheric conditions, fps
c_r	= reverse thrust ratio, $c_r \equiv F_r/\dot{m}U_j$
F_r	= measured reversed thrust, lb _f
f_c	= $\frac{1}{2}$ octave band center frequency, Hz
g_c	= conversion factor, 32.2 lb _m /fps ² /lb _f
k	= conversion factor = 1.356 w/(ft-lb _f /sec)
\dot{m}	= actual mass flow rate, lb _m /sec
n	= number of active vane passages in cascade assembly
OAPWL	= nominal overall sound power level, db re 10 ⁻¹³ w
OASPL	= overall sound pressure level, db re 20 μ N/m ²
OASPL _{max}	= maximum value of OASPL for a given operating condition, db re 20 μ N/m ²
PNL	= perceived noise level, PNdb
PWL	= effective sound power level for each $\frac{1}{2}$ octave band, db re 10 ⁻¹³ w
PR	= nozzle or cascade pressure ratio
SPL	= sound pressure level for each $\frac{1}{2}$ octave band, db re 20 μ N/m ²
U_j	= fully expanded ideal jet velocity, fps
W	= acoustic power, $W = 10^{OAPWL/10} 10^{13}$, w
α	= cascade blade exit angle, deg
θ	= microphone polar angle measured from inlet axis, deg
ρ_o	= air density at ambient conditions, lb _m /ft ³

Introduction

ONE of the aircraft noise sources that can become important in meeting community noise regulations, especially for small airports in heavily populated areas, is the thrust reverser used to reduce ground roll. Studies of reverser noise have not been available in the literature. For this reason, the NASA Lewis Research Center has been conducting an investigation of the noise characteristics of various types of reversers, including target-type reversers for circular and slot nozzles, and cascade reversers with and without shielding.

Results of target-type reverser noise studies have been presented.^{1,4} Preliminary results for cascade reverser noise are presented herein from cold flow model tests of cascade configurations with airfoil-shaped vanes and constant-thickness vanes. Variables investigated in these tests included ratio of cascade exit area to duct inlet area, shape of duct deflector-blocker, and emission arc. These variables were studied over an ideal jet velocity range of 500-1300 fps, corresponding to pressure ratios of 1.15-3.0. Shielding tests on one of the cascade configurations were made with both hard and acoustically soft shields.

Cascade Reverser Models

Cascade reversers consist of a series of vanes located in the walls of the turbine or fan duct upstream of the conventional exhaust nozzle. For reverse thrust, the exhaust nozzle is blocked and the flow deflected through the uncovered cascade vanes. The cascade reverser thus becomes a new exit nozzle and must be designed to match engine operating characteristics. Two cascade reverser models were used in this study.

Airfoil Vane Cascade

The airfoil vane cascade (Fig. 1) had airfoil-shaped, thick, impulse-type vanes with flow inlet and exit angles of 45°. The vanes were set in 8 equal sizes, separate sectors covering a possible total emission arc of 340°. Each sector had 12 vanes. An axially adjustable conical blocker allowed selection of the number of blades to be made active. Each cascade sector (42.5° arc) could be replaced with a blanking plate. The minimum flow area for each passage, A'_{min} (about 0.75 of the cascade exit area) occurs near the inlet edge of the vanes. This cascade therefore is in effect a convergent-divergent flow passage. Dimensional details appear in Fig. 1 and in Ref. 5.

Presented as Paper 74-46 at the AIAA 12th Aerospace Sciences Meeting, Washington, D.C., January 30-February 1, 1974; submitted March 6, 1974; revision received September 3, 1974.

Index categories: Aircraft Noise, Powerplant; Aircraft Noise, Aerodynamics (Including Sonic Boom); Aircraft, Deceleration Systems.

Aerospace Engineer, Member AIAA.

6-in. standard pipe (6½ in. o.d.). There were 5 parallel passages in each cascade sector. The vanes were of the impulse type with inlet and outlet angles of 30° to the axis. Other dimensions appear in Fig. 3. The exit area, A_{ex} is the minimum flow area for this cascade (0.65 of the inlet area). Thus, the flow passage corresponds aerodynamically to a convergent nozzle. This small exit-to-inlet area ratio cascade would be applicable to engines with a high nozzle pressure ratio such as 2.5.

The thin-vane cascade was tested with two different flow blockers, a flat rear blocker set about 8 in. downstream of the cascade sector, and a fixed deflector-blocker consisting of a solid cylindrical insert with two plane 30° wedge cuts ending even with the cascade rearmost vanes. No adjustment of the blocker position was possible on this design.

Test Facility and Procedure

Rigs

The cascade reverser experimental data were obtained on two separate flow systems. The noise data were taken on an acoustic rig designed to minimize internal noise and instrumented to obtain detailed acoustic data. Another airflow rig was used to obtain exhaust-jet velocity surveys and data on thrust-reversal performance. The airflow rig was essentially as described in Ref. 6, but for the thrust reverser tests the piping was extended far enough to let the existing velocity survey equipment be used in the reserved jets. Reverse thrust was measured by preloading the axial thrust load cell with 500 lb in weights hung from pulleys.

The acoustic rig is shown in Fig. 4. Compressed air from a 140 psi abs source was supplied to the reverser at near ambient temperature (60-80° F) by an 8-in. diam pipe equipped with a flow-measuring orifice, a remotely operated flow control valve, a noise muffler, and a straight run ending at the nozzle, which was 63 in. above ground level.

The noise data were measured by nine condenser microphones with individual wind screens, located on a semicircle of 15 ft radius centered on the middle of the reverser exit plane. These microphones were spaced at 20° increments from $\theta = 20-180^\circ$ from the pipe inlet centerline, at the same height above the smooth asphalt surface as the pipe centerline.

Procedure

Aerodynamic and acoustic tests were performed on all the cascade reverser configurations. Flow data were recorded for all tests, as well as pressure and temperature readings. In the aerodynamic tests, axial force measurements to determine reverse thrust were also taken. In the acoustic tests, after flow conditions had stabilized, flow parameters and atmospheric conditions were recorded together with the noise data from each of the nine microphones. The noise data were analyzed directly by use of a 1/3-octave band analyzer and recorded on magnetic tape for computer processing.

The 1/3-octave-band analyzer yielded the sound pressure level (SPL) in each band from 50-20 000 Hz. These data were corrected for atmospheric absorption, and the overall sound pressure level (OASPL) was computed for each microphone. The nominal spectral sound power level (PWL) and the nominal overall sound power level (OAPWL) were obtained

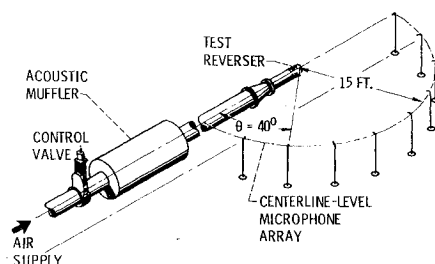


Fig. 4 Schematic diagram of acoustic rig.

by integration. These power levels are termed "nominal" since the noise measured is a function of the azimuthal angle while the integration assumes symmetry about the jet axis. Detailed ground reflection corrections are not made herein. The microphone data are corrected only for this facility's high-frequency asymptotic reflection of 2.2 db.

Results and Discussion

Aerodynamic and acoustic results obtained with the cascade thrust reversers are presented in graphical form. In addition, complete tables of 1/3-octave band noise spectra for all microphone locations are available, upon request, from the authors.

Aerodynamic Results

Reverse thrust ratios are plotted against stagnation Mach number U_j/c_o in Fig. 5 for all the configurations tested. The reverse thrust ratio c_r is the ratio of the measured reverse thrust, F_r , to the forward thrust possible from the same mass flow rate at the ideal jet velocity $\dot{m}U_j$.

The airfoil-vaned cascade, as shown in Fig. 5a and b, had reverse thrust ratios ranging between 0.6 and 0.7, depending on the stagnation Mach number. The one exception was the 5-vane cascade with a 340° emission arc which had higher values at the lower values of U_j/c_o . Traverses taken at the cascade exits showed all but the 340° emission arc configuration had flow leaving the blades at 45° from the axis, indicating good flow attachment to the blades. However, the flow from the 340° emission arc cascade configuration ($A_{ex}/A_{in} = 1.25$) was found to be attached to the outside wall of the inlet pipe. This attachment was responsible for the odd variation in reverse thrust ratio shown for this case in Fig. 5a.

The thin-vaned cascade reversers had a markedly lower reverse thrust ratio than the airfoil-vaned cascades. The application of the deflector-blocker to the thin-vaned cascade with flat blocker improved its reverse thrust ratio from approximately 0.35 (same as obtained with the V-gutter target reverser of Ref. 3) to about 0.45. In both cases velocity traverses taken at the exit of the cascades indicated flow separation, with jets exiting at angles of around 50° from the axis rather than at the vane exit angle of 30°. The low level of reverse thrust from the thin-vane cascade is most likely caused by flow separation resulting from the poor flow area distribution along the vane chord.

Sound Power Level

Normalized OAPWL's are shown in Fig. 6 as a function of stagnation Mach number for all airfoil cascade reverser configurations tested. The OAPWL is shown normalized by $\rho_o A_e U_j^3$ and plotted against the stagnation Mach number U_j/c_o . The area used in this term A_e is the equivalent area required to flow the measured mass flow rate at the ideal fully expanded jet velocity. The values of A_e are a function of operating conditions and are shown in Table 2 as ratios of exit area, A_e/A_{ex} . There is an obvious change in the slope of the

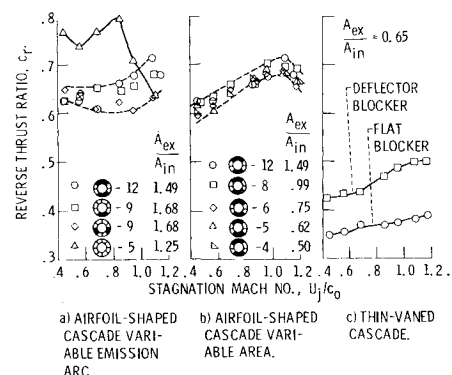


Fig. 5 Cascade reversed thrust coefficient as a function of stagnation Mach number U_j/c_o .

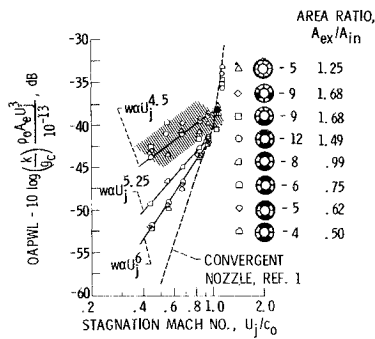


Fig. 6 Normalized overall sound power level for airfoil-shaped cascade reverser.

curves for the different variations as well as a change in level. The shift in slope seems to be related to the exit-to-inlet area ratio.

The cascades tested at variable emission arc with exit-to-inlet area ratios about 1.25 have the highest noise levels. All four of the cascade configurations in this group deviate from a constant exponent relation with Mach number with no apparent separation between the individual configurations.

The cascade configurations with a constant circumferential emission arc of 170° showed a marked change in slope and level when the exit-to-inlet area ratio decreased below a value of around 1.0. At a value of 0.99 the acoustic power became a very orderly function of the $5\frac{1}{2}$ power of velocity. A decrease of the area ratio to 0.75 reduced the acoustic power still lower and made it proportional to the sixth power of the velocity. A further decrease in the area ratio as low as 0.50 did not change the normalized OAPWL. It is also noted that as the stagnation Mach number approaches 1.0, the reverser nor-

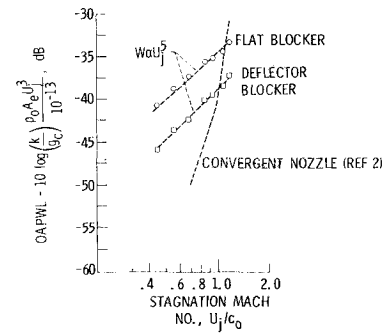










Fig. 7 Normalized overall sound power level for thin-vaned cascade reversers.

malized OAPWL follows very closely the relationship obtained in Ref. 1 for a convergent nozzle alone.

The nominal overall sound power level (OAPWL) for the thin-vaned cascade reversers is shown in Fig. 7. Comparisons of Figs. 6 and 7 shows that the airfoil-shaped cascade reverser with exit-to-inlet area ratio smaller than 1 has the lowest normalized OAPWL of all the cascades and are also lower than any of the target reversers tested.¹⁴ Since the reverse thrust ratio for the small area ratio airfoil-bladed cascade reverser is as high or higher than for any other reverser (Fig. 5), these configurations appear to have the most satisfactory reverse thrust-to-noise ratio of all the reverser models investigated. However, as previously mentioned, the cascade type reversers must be designed to match engine operating characteristics.

The sound power level data for the 170° emission arc cascades shown in Fig. 6 have been replotted in Fig. 8 to show the effect of cascade area ratio. Values of OAPWL are plotted as a function of area ratio A_e/A_{in} for constant values of

Table 2 Ratio of effective area to exit area, A_e/A_{ex} , for the various cascade configurations

Pressure ratio, P.R.	1.15	1.25	1.40	1.72	2.00	2.50	3.00
Stagnation Mach number, U_j/c_0	.44	.55	.67	.85	.95	1.07	1.16
Cascade type	A_e/A_{ex}						
<u>Thin vaned</u>							
With flat blocker	0.844	0.859	0.875	0.911	0.943	1.009	1.069
With deflector-blocker	.877	.882	.894	.925	.933	.999	1.068
<u>Airfoil vaned</u>							
 - 5	0.733	0.718	0.707	0.693	0.700	0.725	----
 - 9	.554	.554	.551	.539	.548	.567	----
 - 9	.586	.578	.583	.565	.562	.583	----
 - 12	.560	.564	.561	.565	.590	.607	0.640
 - 8	.656	.655	.655	.657	.672	.713	.756
 - 6	.684	.679	.692	.692	.704	.747	.796
 - 5	.687	.694	.694	.704	.716	.755	.812
 - 4	.695	.706	.702	.707	.727	.768	.817

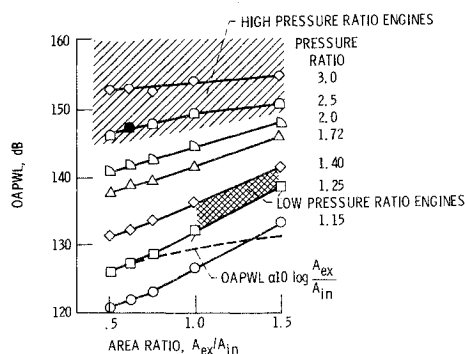


Fig. 8 Overall sound power level as a function of exit area ratio, A_{ex}/A_{in} for airfoil vaned cascade. Emission arc; 170° ; A_{in} ; 21.5 in.^2 .

pressure ratio. In addition, a reference linear variation of acoustic power with exit area is shown by the dashed line. For area ratios up to $A_{ex}/A_{in} = 0.75$, the OAPWL is essentially proportional to the area ratio over the pressure ratio range of 1.15-3.0. However, as the area ratio increases beyond 0.75 the OAPWL increases faster than the area ratio for pressure ratios between 1.15 and 2.0. The area ratio effect on OAPWL is the greatest at $PR = 1.15$ and decreases as the pressure ratio increases. At pressure ratios about 2.0 the OAPWL is again directly proportional to the area ratio throughout the area ratio range.

The lower crosshatched section shown in Fig. 8 represents the expected pressure ratio-area ratio zone of interest for low pressure fans applicable to externally-blown-flap STOL engines. The upper crosshatched section is representative of the operating zone for engine exhaust ducts at high pressure ratio, such as used in CTOL engines, and such STOL applications as the augmentor wing and core engines.

Directivity

Typical OASPL directivity plots are shown in Fig. 9 for the airfoil-vaned cascade with 170° emission arc and area ratios of 0.5 and 0.99. The difference between the OASPL at a given angle and the maximum OASPL is plotted as a function of polar angle. As with all reversers tested the OASPL distribution is much more omnidirectional than for pure jet noise. The greatest deviation from the maximum OASPL shown in Fig. 9 is $5\frac{1}{2} \text{ db}$. The directivity is a function of the exit ideal jet velocity, which was also the case for the thin-bladed cascade reverser. For U_j/c_o less than 0.67, the peak OASPL occurs at $120\text{-}140^\circ$ from the inlet axis, which is nearly 90° from the direction of the exiting jets. At the higher velocities (U_j/c_o above 0.95), the peak OASPL shifts to

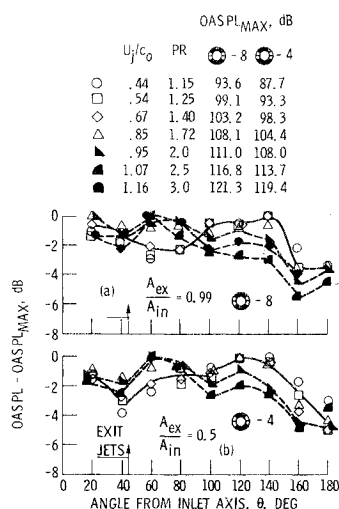


Fig. 9 Noise directivity of airfoil-shaped cascade reverser. Emission arc = 170° .

angles of $20\text{-}60^\circ$ from the inlet axis, which is approximately $15\text{-}20^\circ$ on either side of the exiting jets. At intermediate velocities (U_j/c_o between 0.67 and 0.95), the directivity is more uniform.

These directivity shifts imply that both surface-generated noise (dipole) and jet-generated noise (quadrupole) exist, with surface-generated noise controlling at the low velocities and jet noise at the high velocities. The shifts start before ideal sonic conditions are reached. The airfoil-shaped cascade configurations with large area ratios (directivity plots not shown) present similar trends.

Spectra

A direct comparison of the spectra for the same reverser configuration at the three angles at which the maximum OASPL occurs for some velocity is shown in Fig. 10 for 3 velocity levels. The case shown is for the cascade with 170° emission arc and 8 blades (exit-to-inlet area ratio of 0.99). The shape of the spectra at the 140° angle changes very little over the range of U_j/c_o ; it is always dominated by the high frequency noise. The spectra at the other two angles (20° and 60° from the inlet axis) change appreciably with a change in U_j/c_o . At the low value of U_j/c_o the spectra are high-frequency dominated having a spectral shape similar to that at 140° . As the velocity increases, sound pressure levels for the lower frequencies increase more rapidly than for the high frequencies until they become dominant. At the $20\text{-}60^\circ$ angles, for instance, the 1 kHz frequency increased as the 8th power of velocity, while the 8 kHz frequency increased as the 6th power of the velocity. The implication is that at low velocities the cascade reverser noise is dominated by high frequency, dipole-type noise throughout the whole radiation arc, and as the velocity increases the jet-type noise becomes important at angles near the jet exit. At the higher velocities, jet noise controls the spectra, except that the high frequency roll-off rate is reduced.

Figure 11 shows noise spectra for the airfoil-shaped cascade reverser with a constant 170° emission arc and variable area ratios from 0.5-1.49. The spectra shown are for a pressure ratio of 1.25 ($U_j/c_o = 0.55$) in the direction of maximum OASPL. The shape of the spectra is similar for all the con-

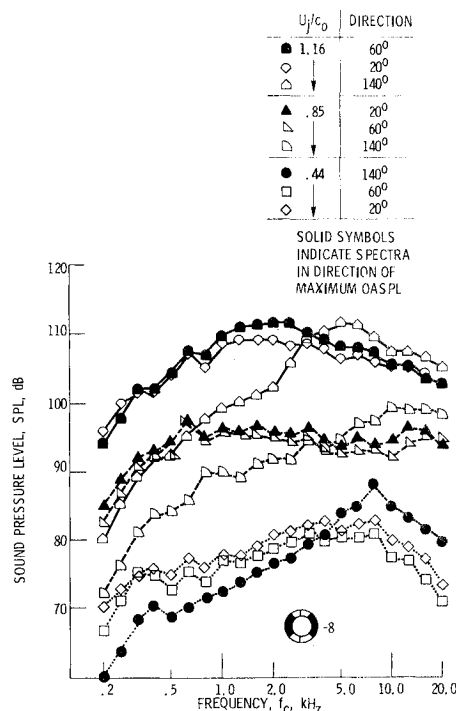


Fig. 10 Comparison of SPL spectra at angles of 20° , 40° , and 140° for airfoil-shaped cascade reverser. 170° emission arc; 8 vanes; A_{ex}/A_{in} , 0.99.

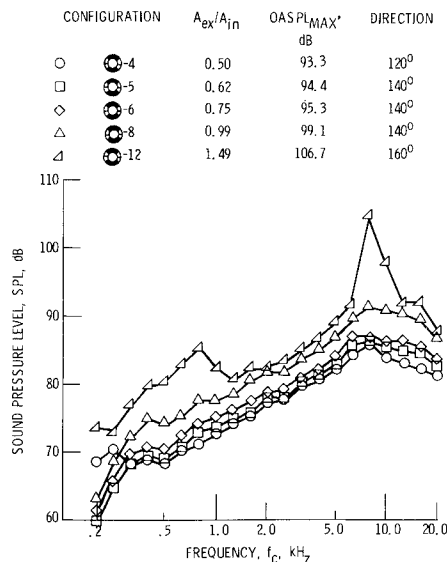


Fig. 11 Comparison of sound pressure level spectra in direction of maximum OASPL for airfoil-shaped cascade reverser. 170° emission arc, variable A_{ex}/A_{in} ; $U_j/c_o = 0.55$; $PR, 1.25$.

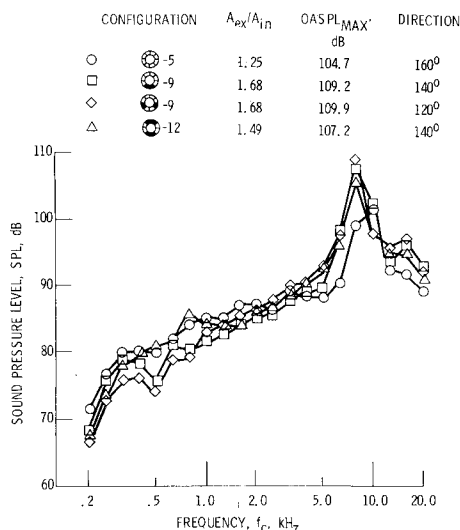


Fig. 12 Comparison of sound pressure level spectra in direction of maximum OASPL for airfoil-shaped cascade reverser with different emission arcs. $A_{ex}/A_{in} \geq 1.25$. Effective Mach number, $U_j/c_o = 0.55$, $PR, 1.25$.

figurations up to an area ratio of 0.99 (8 vanes) like those shown in Fig. 10. For the area ratio 1.49 case (12 vanes), very high level narrow-band noise appears at the 0.8 and 8 kHz $\frac{1}{2}$ octave bands. The narrow band noise at 8 kHz completely dominates the noise level. This narrow band noise appears in the spectra for all the airfoil cascade reverser configurations tested at the area ratios larger than 1, as shown in Fig. 12. The narrow-band noise was the dominant source of noise for the large exit-to-inlet area ratio airfoil cascades at the lower pressure ratios, but is not noticeable at pressure ratios above 1.72 ($U_j/c_o > 0.85$). No tones were observed with the thin vane cascade ($A_{ex}/A_{in} = 0.62$).

Although the exact cause of the high-frequency tones in Fig. 12 is not known, there are a number of possible mechanisms that could give rise to such tones: mechanical resonance, subsonic feedback (screech), trailing vortex sheet, and flow oscillations producing fluctuating vane lift. Most of these sources would be suppressed with the onset of choked flow or sonic velocities. However, the reason for the appearance of tone noise only for the high area ratio configurations is not clear. For area ratios greater than 1.0, the

cascade tends to represent a diffuser with parallel flow passages. Such a configuration may be susceptible to flow instabilities both within a vane passage and from passage to passage. However, whatever the source, the high frequency tones are the cause of the irregular variation of acoustic power with velocity level previously discussed (Fig. 6) for the airfoil-shaped cascade reverser configuration with area ratio greater than one.

Sideline Shielding

Tests were conducted using the thin-vaned cascade reverser with the deflector blocker to determine the effectiveness of shields or side plates on deflecting noise away from the sideline, thereby reducing the noise level in that direction. The shields used are shown in Fig. 13. These shields were tested with and without a 1-in. layer of broadband (bulk type) acoustic insulation over the plates, as well as over the duct cowl. The plates shielded the line of sight from the cascade to the sideline at angles from 90-180° from the inlet axis. The actual test plates were long with respect to the cascade body to allow mounting from the rear face of the cascade assembly. The shielding characteristics should be the same for a corresponding flight-size shield as shown by dotted lines in Fig. 13. However, caution must be exercised in sizing and spacing the shields. If the shields are placed too close to the exiting jets they might introduce additional sources of low frequency noise as discussed in the shielding studies of Ref. 7.

Shielding tests results are shown in Fig. 14 for two different pressure ratios. The hard shields gave an appreciable reduction in OASPL for angles greater than 80° from the inlet axis. As much as a 5 db reduction was obtained at angles of 100° and 180°. At low angles, the OASPL actually increased somewhat due to reflection from the shields. Addition of acoustic insulation to the shielding plates and cowl produced a significant reduction in the noise at angles smaller than 120°. However, the effect of the insulation at angles greater than 120° was relatively minor.

Comparison of Reverser Sideline Perceived Noise Level at Aircraft Scale

Estimates of perceived noise levels at the 500-ft sideline for sizes suitable to two distinct STOL aircraft applications have been made. One of the applications was to a high pressure ratio exhaust duct, the other to a low pressure ratio exhaust duct. In all cases, scaling was made to an arbitrary total engine forward thrust of 19,000 lb.

Assumptions made on scaling the reverser data to aircraft size were that frequency varies inversely with exhaust equivalent diameter and intensity varies directly with the

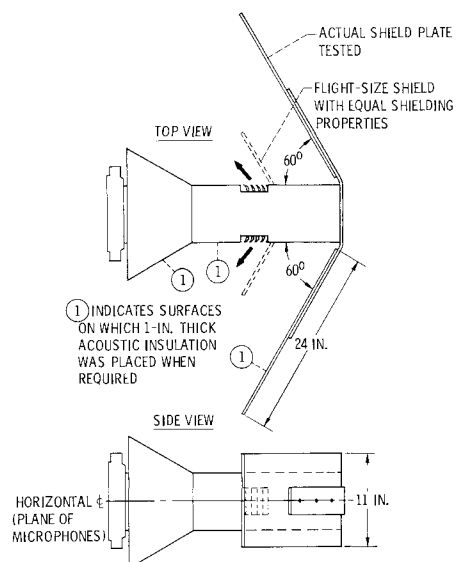


Fig. 13 Sketch of shields used on cascade with thin vanes.

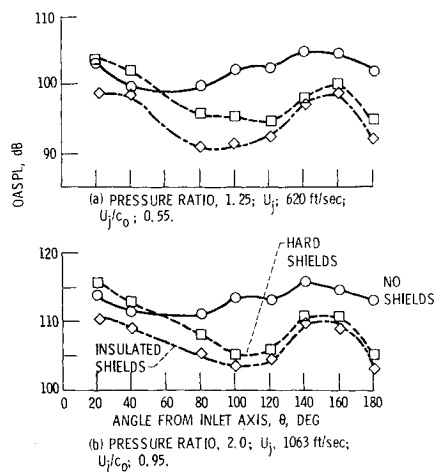


Fig. 14 Effect of sideline shielding on overall sound pressure level for thin-vaned cascade with deflector blocker.

square of the equivalent diameter. A high frequency roll-off of 2 db/ $\frac{1}{3}$ -octave band was assumed in order to estimate the SPL's for those frequency bands where there were no data due to scaling shifts. No specific aircraft configuration was considered, and no allowance was made for reflection from the aircraft. However, the ground reflections of the experimental data were included without correction. The data were corrected for atmospheric attenuation according to Ref. 8; no correction was made for extra ground attenuation. The perceived noise level for each angle was then calculated according to Ref. 9.

High Pressure Ratio Engine

In order to compare results directly with those presented in Ref. 4 for a V-gutter target reverser, a 19,000-lb-thrust engine exhaust with a 2.5 nozzle pressure ratio ($D_e = 28$ in.) was chosen as the high pressure ratio engine for scaling purposes. The resulting perceived noise levels at the 500-foot sideline are shown in Fig. 15. The PNL's are shown for the V-gutter target reverser of Ref. 4 together with those for two cascade reversers, the thin-vane cascade reverser with deflector blocker ($A_{ex}/A_{in} = 0.65$, 120° emission arc) and the airfoil-vane reverser with 170° emission arc and 6 vanes ($A_{ex}/A_{in} = 0.75$).

Figure 15a presents results for operation at full pressure ratio (2.5) which represents an ideal velocity of 1188 fps. The cascades would seem about 2-2.5 PNdb louder than the V-gutter reverser. However, for these not-very different noise levels, the cascade reversers yield larger reversed thrust than the V-gutter reverser. This increase is about 35% for the thin bladed cascade and nearly 85% for the airfoil bladed cascade reverser.

Re-evaluating the sideline PNL's for these same configurations on the basis of the same exhaust duct size as before but at the reduced ideal velocities (throttle settings) necessary to produce equal reversed thrust, the results of Fig. 15b are obtained. The thin-vane cascade reverser is about 1 PNdb quieter and the airfoil-vane cascade reverser is 5 PNdb quieter than the V-gutter reverser. However, even the quietest of all these noise levels still show PNL values well above the 95 PNdb design goal for a STOL aircraft for a considerable distance along the sideline (single engine goal would be about 2-6 PNdb less, depending on number of engines and aircraft configuration).

Figure 16 shows the sideline shielding results with the thin vane cascade ($A_{ex}/A_{in} = 0.65$) scaled to the same engine application described in Fig. 15b. The hard shields reduced the maximum sideline PNL by 6 PNdb while the insulation reduced it an additional 2 PNdb. Even with the shield, the single-engine maximum PNL is still well above the STOL aircraft noise goal of 95 PNdb. However, the length along the sideline (measure of exposure time) for which the PNL is above the goal value has been reduced.

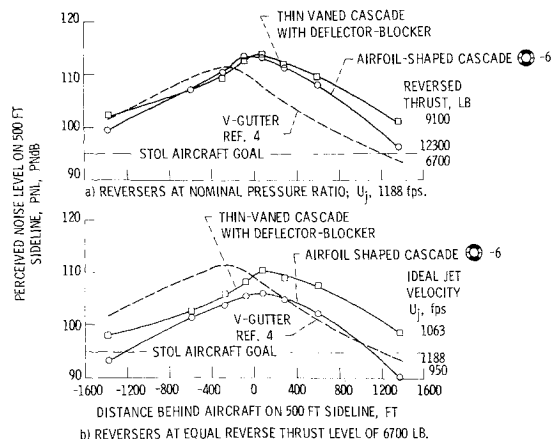


Fig. 15 Sideline noise for different reversers applied to a 19,000-lb-thrust engine. Nominal full throttle pressure ratio: 2.5; forward thrust nozzle equivalent diameter: 28 in.

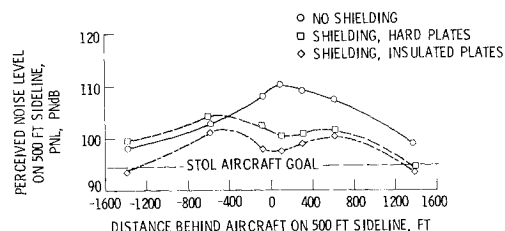


Fig. 16 Effect of sideline shields on thin-vaned cascade reverser sideline noise scaled to a 19,000-lb-thrust 2.5 pressure-ratio engine. Partial throttle operation for reverser thrust, 6700 lb U_j 1063 fps, $PR = 2.0$.

Although sideline shielding tests were not run with the airfoil vane cascade, an estimation can be made concerning the resultant perceived noise level for an airfoil vane cascade reverser with a treated sideline shield. If the effect of the shield on the PNL pattern were the same as for the thin vane cascade (Fig. 16), a corresponding decrease in maximum PNL due to shielding would be obtained (8 PNdb). This would still produce a maximum PNL for the shielded airfoil vane cascade of Fig. 15b around 4 PNdb above the 95 PNdb goal, but it would decrease appreciably the exposure time above that PNL value at the sideline.

The calculation of the previous figures were based on a ratio of reverse thrust to ideal exhaust thrust of around 0.35 for a high-pressure ratio exhaust. If a higher value of reverse thrust ratio were required, perhaps 0.5, the target-type reverser would not be capable of producing the required reverse thrust. Furthermore, the cascade-type reversers would have to operate at higher pressure ratios (higher ideal exhaust velocities) with resulting higher noise levels. However, required reverse thrust ratios less than the example of 0.35 would be very beneficial in reducing perceived noise because of reduced operating pressure ratios. Large reductions in noise would result in view of the steep variation of sound power with exhaust velocity (U_j) for low nominal area ratio cascades (Figs. 6 and 7).

Low Pressure Ratio Engine

The low pressure ratio engine chosen for scaling was a 19,000 lb thrust engine with a 1.25 nozzle pressure ratio ($D_e = 59.7$ in.). This would be representative of the fan stage of a high-bypass turbofan engine. Because of the low pressure ratio available in such engines, the value of A_e/A_{in} for suitable cascade reversers would probably be about 1 or greater, as shown by the shaded area in Fig. 8. The cascades chosen for scaling to the low pressure ratio engine size were the airfoil-vane cascade reversers with 170° emission arc and $A_{ex}/A_{in} = 0.99$ and 1.49 (8 and 12 vanes, respectively). These

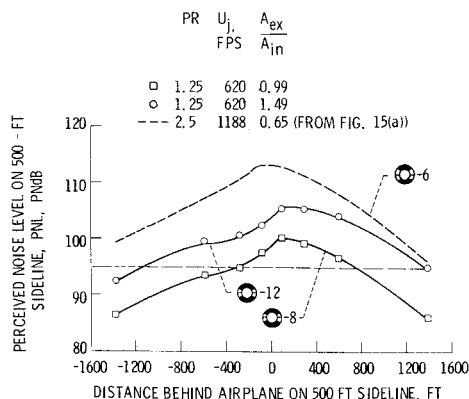


Fig. 17 Sideline noise for airfoil-shaped cascade reversers applied to a 19,000-lb-thrust fan duct. Nominal full-throttle pressure ratio = 1.25; forward-thrust nozzle equivalent diameter = 59.7 in.; reverse thrust = 12,300 lb.

two airfoil-vane cascades configurations are indicated in Fig. 8 by tailed symbols. The airfoil-cascade that was scaled to the high pressure engine in the previous calculation is shown by the solid symbol in that figure.

The scaled PNL's for both airfoil-shaped cascade reversers are shown in Fig. 17. The PNL along the 500-ft sideline for the airfoil cascade scaled to the high pressure ratio engine for the same reversed thrust (12,300 lb) is shown as a dashed line for comparison. The $A_{ex}/A_{in}=0.99$ airfoil cascade, unshielded, was about 12 PNdB quieter than the airfoil cascade reverser for the high pressure ratio engine. Assuming the same relative results as in Fig. 16, the addition of sideline shields would then reduce the peak sideline PNL to around 3 PNdB below the goal of 95 PNdB.

The calculation of Fig. 17 was for a ratio of reverse thrust to maximum engine thrust of 0.65, which is the value of c_r achieved with the airfoil vane cascade. However, an aircraft application would probably require a lower value of reverse thrust. For example, if the part throttle operating point was reduced to a fan pressure ratio of 1.15, the ratio of reverse thrust to maximum engine thrust would be around 0.4 (assuming no change in cascade thrust coefficient). According to Fig. 8, a reduction in pressure ratio from 1.25-1.15 produced around a 5.5 db reduction in overall sound power level for cascade area ratios between 1 and 1.5. Assuming as a first approximation that this decrease in OAPWL would be reflected as an equivalent decrease in PNL, then the maximum sideline PNL for the airfoil cascade ($A_{ex}/A_{in}=0.99$) part-throttle case might be at the 95 PNdB level. With the use of sideline shields, the maximum PNL could be reduced to around 8 PNdB below the goal value. Thus, it appears possible to obtain thrust reversers for low-pressure ratio engine applications that have a potential for meeting the 95 PNdB aircraft noise goal.

The above comparisons are valid specifically for the assumptions made. However, caution should be exercised as some of these assumptions may not be applicable when limited by mechanical feasibility considerations. For instance, the geometric scaling assumption requires that the cascade vanes for the engine with $D_e=59.7$ in. must have a 7-in. chord which would require an increase of over 1 ft on the duct diameter just for stowing purposes. If the vanes dimensions are not increased in the same proportion as the cascade area, the dipole noise (controlled by vane dimensions) and the jet noise (controlled by total cascade area) should scale by different values, resulting in changes in spectral distribution and atmospheric attenuation. These changes will, of course, alter the sideline PNL obtained.

Conclusions

The cascade configurations tested point out the difficulties of achieving low noise goals with thrust reversers for STOL applications. Based on the cold-flow model test results and the preliminary analysis reported herein, it may be possible to obtain thrust reversers (airfoil-shaped cascade configuration plus sideline shielding) that approach the 95 PNdB sideline goal only with high bypass (low pressure ratio) exhausts. In general, reductions in the required reverse thrust will allow large reductions in reverser sideline noise by allowing operation at partial throttle settings. In addition, further investigation is useful in identifying cascade reverser geometry variables that will produce minimum perceived noise.

References

- Gutierrez, O.A. and Stone, J.R., "Preliminary Experiments on the Noise Generated by Target-Type Thrust Reverser Models," TM X-2553, May 1972, NASA.
- Stone, J.R. and Gutierrez, O.A., "Target-Type Thrust Reverser Noise," *Journal of Aircraft*, May 1973, pp. 283-288; also, TM X-68082, Aug. 1972, NASA.
- Stone, J.R. and Gutierrez, O.A., "Small-Scale Noise Tests of a Slot Nozzle with V-Gutter Target Thrust Reverser," TM X-2758, April 1973, NASA.
- Stone, J.R. and Gutierrez, O.A., "Noise Tests of a High-Aspect-Ratio Slot Nozzle with Various V-Gutter Target Thrust Reversers," TM X-71470, Oct 1973, NASA.
- Dietrich, D.A. and Luidens, R.W., "Experimental Performance of Cascade Thrust Reversers at Forward Velocity," TM X-2665, Feb. 1973, NASA.
- Huff, R.G. and Groesbeck, D.E., "Splitting Supersonic Nozzle Flow into Separate Jets by Overexpansion into a Multilobed Divergent Nozzle," TN D-6667, March 1972, NASA.
- von Glahn, U., Goodykoontz, J., and Wagner, J., "Nozzle Geometry and Forward Velocity Effects on Noise for CTOL Engine-Over-the-Wing Concept," TM X-71453, Oct. 1973, NASA.
- "Noise Standards: Aircraft Type Certification," *Federal Aviation Regulations*, Vol. III, Pt. 36, 1969.
- "Definitions and Procedures for Computing the Perceived Noise Level of Aircraft Noise," *Aerospace Recommended Practice 865A*, Aug. 1969, Society of Automotive Engineers, New York.